

1 Traveling planetary-scale Rossby waves in the winter
2 stratosphere: The role of tropospheric baroclinic
3 instability

Daniela I.V. Domeisen,¹ R. Alan Plumb¹

¹Department of Earth, Atmospheric and
Planetary Sciences, Massachusetts Institute
of Technology, Cambridge, Massachusetts,
USA.

4 We report results from a series of runs of a simplified ("dynamical core")
5 general circulation model, aimed at understanding the generation of trav-
6 eling planetary-scale Rossby waves in the winter stratosphere. The model has
7 no topographic or other external wave forcing. When the model is truncated
8 to permit only waves with zonal wave number 1 or 2, the long waves are found
9 to be stronger than when zonally shorter waves are included, leading to a
10 more active stratosphere. On the basis of these results and the diagnosed wave
11 properties, we conclude that (consistent with an earlier suggestion by Hart-
12 mann) traveling long waves are generated primarily by tropospheric baro-
13 clinic instability rather than by nonlinear interactions among synoptic-scale
14 eddies.

1. Introduction

15 Traveling planetary-scale Rossby waves are observed in the extratropical stratosphere
 16 of both hemispheres. They are especially prominent in the Southern Hemisphere, while
 17 quasi-stationary waves dominate in the Northern Hemisphere due to the presence of
 18 stronger surface excitation. Several mechanisms have been proposed to be able to force
 19 large amplitude traveling waves in the absence of strong surface forcing: Hartmann [1979]
 20 suggested a generation of traveling waves by Charney-type baroclinic instability of zonal
 21 wave-2 in the troposphere. Scinocca and Haynes [1998] suggested nonlinear interactions
 22 among synoptic-scale baroclinic eddies in the troposphere as the origin of stratospheric
 23 traveling waves. Kushner and Polvani [2005] ascribed waves (and a major stratospheric
 24 warming produced by these waves) in a spectral core model with no longitudinally varying
 25 forcing to the latter mechanism.

26 We here report results from a similar spectral core model without external wave forcing:
 27 Suppressing synoptic-scale eddies by a severe spectral truncation yields an increase in
 28 planetary wave fluxes into the stratosphere. The absence of synoptic eddies necessary to
 29 excite planetary-scale motion according to the Scinocca and Haynes [1998] mechanism,
 30 together with the characteristics of the modeled wave structure, leads us to conclude that
 31 the model's planetary-scale waves are produced primarily by Charney-type baroclinic
 32 instability in the troposphere, as Hartmann suggested.

2. Model Setup

33 The model used in this study is the spectral core of a general circulation model of
 34 intermediate complexity at T42 resolution as specified in Polvani and Kushner [2002],

35 except the present model is in hybrid $\sigma - p$ coordinates. This setup includes a linear
36 relaxation towards a zonal mean equilibrium temperature profile which corresponds to
37 the Held and Suarez [1994] profile in the troposphere with an asymmetry about the
38 winter hemisphere, and a cooling over the winter pole in the upper stratosphere. We use
39 a $\gamma=4\text{K/km}$ lapse rate for the winter stratospheric cooling (for the definition and use of
40 γ see Polvani and Kushner [2002]), which corresponds to a strong Southern Hemisphere -
41 like polar vortex. The model runs have no seasonal cycle and are run in perpetual winter
42 conditions.

43 We are presenting a comparison of two model runs of 10,000 days length each: Both
44 runs use the above setup with no longitudinally varying forcing. We then compare the
45 control run to a truncated run as explained below.

46 For the truncated run, the only difference to the control run is a truncation in wave num-
47 ber space to zonal wave-1 and wave-2 and a mean flow only. There is no such truncation
48 in the meridional direction.

49 For completeness, an additional model run was performed which was truncated to zonal
50 wave-2 and a mean flow only. It confirms the conclusions made from the above runs as
51 described in the Results section.

3. Results

52 The control run yields a very strong polar vortex with mean winds around 100m/s at
53 its center, with a standard deviation of 5m/s. Stratospheric variability is significantly
54 reduced as compared to the real atmosphere, and no stratospheric sudden warmings are

55 observed (Figure 1a shows a representative excerpt from the control run). The time series
 56 of the Eliassen-Palm flux (EP flux) entering the stratosphere looks noisy (Figure 1b).

57 Truncating the model to zonal wave-1 and wave-2 yields a significant increase in strato-
 58 spheric variability (Figure 2a). In particular, large amplitude warmings occur intermit-
 59 tently associated with large excursions in the EP fluxes (Figure 2b).

60 In order to understand the differences in wave behavior, time-averaged vertical EP fluxes
 61 divided into planetary-scale (zonal wave-1 and wave-2) and shorter (wave-3 and higher)
 62 waves are examined. In the control run the long waves determine the wave flux in the
 63 stratosphere as expected (Figure 3b), while the EP flux in the troposphere is dominated
 64 by higher wave numbers (Figure 3c), with the long waves accounting for only about 10%
 65 of the tropospheric wave flux.

66 If these shorter waves are responsible for the upward long-wave EP flux in the strato-
 67 sphere, we would expect the long-wave flux to vanish when smaller scale waves are inhib-
 68 ited in the model atmosphere. In the truncated run, however, the long-wave flux actually
 69 strengthens, not only in the stratosphere, but also in the troposphere (Figure 4b). Results
 70 from the additional model run truncated to zonal wave-2 and a mean flow yield the same
 71 results, in fact this run exhibits slightly stronger stratospheric variability than the run
 72 truncated to both wave-1 and wave-2.

73 Since in the truncated run, synoptic motions are nonexistent, nonlinear interaction be-
 74 tween them cannot be responsible for forcing the long waves. Tropospheric baroclinic
 75 instability of the long waves themselves, as suggested by Hartmann [1979], must be re-
 76 sponsible for the generation of these waves.

77 Instability of the long waves is enhanced in the truncated run since the suppression of
 78 the synoptic-scale waves increases the baroclinicity of the troposphere (compare the lower
 79 tropospheric wind shear in Figures 3a and 4a).

80 In addition, the characteristics of the waves indicate their origin from baroclinic insta-
 81 bility. Waves with long zonal wavelengths can become synoptic-scale in terms of their
 82 total horizontal wavelength by adopting a large meridional wavenumber, and by being
 83 confined to high latitudes [Hartmann, 1979], and can be classified as Charney modes.
 84 Figure 5 shows a comparison between the meridional length scale of zonal wave-2 for the
 85 two presented runs. The variable shown is the Southern Hemisphere meridional length
 86 scale L_y of the wave scaled by earth's radius a , defined here, assuming geostrophic balance,
 87 as

$$\frac{L_y}{a} = -\frac{g}{f a} \sqrt{\frac{\langle \overline{\phi_2'^2} \rangle}{\langle \overline{u_2'^2} \rangle}} \quad (1)$$

88 where f is the Coriolis parameter, ϕ_2' are the geopotential wave-2 zonal anomalies, u_2' are
 89 the wave-2 zonal anomalies of zonal wind, an overbar denotes a zonal average and $\langle . \rangle$
 90 denotes a time average. Both the control run and the truncated run indicate a small
 91 meridional scale, $L_y \leq 0.2a$, of the wave in the troposphere. The scale increases with
 92 height as required for propagation [Charney and Drazin, 1961].

93 Since there is no external forcing in these experiments, quasi-stationary waves are es-
 94 sentially absent. In both the control and the truncated runs zonal wave-2 exhibits inter-
 95 mittent occurrences of systematic eastward propagation with periods of order 10 days
 96 interspersed with episodes of slower propagation in either direction. Figure 6 shows spec-

97 tra of geopotential height amplitude of wave-2 at 189hPa. There are some differences
 98 between the characteristics of the control and the truncated run: In the latter, there is a
 99 spectral peak of about frequency 0.08/day, whereas in the control run there is broad low
 100 frequency variability without a clear peak.

4. Conclusions

101 In the absence of a stationary planetary-scale tropospheric forcing such as topography or
 102 a heat source, the generation of zonally long waves penetrating the stratosphere has been
 103 attributed to nonlinear wave-wave interaction between synoptic-scale baroclinic eddies in
 104 the upper troposphere [Scinocca and Haynes, 1998].

105 However, stratospheric variability in a spectral core model with no longitudinally vary-
 106 ing forcing increases when synoptic variability is eliminated, indicating that another mech-
 107 anism, namely baroclinic instability of long waves, is responsible for forcing the long waves
 108 propagating into the stratosphere, as suggested by Hartmann [1979]. This hypothesis
 109 is supported by multiple indicators: wave-wave interaction among synoptic-scale waves
 110 is inhibited and therefore not responsible for causing the planetary wave flux into the
 111 stratosphere, interaction between planetary-scale waves weakens the wave flux into the
 112 stratosphere as confirmed in an additional experiment truncated to zonal wave-2 only,
 113 and the small meridional scale of the waves in the troposphere indicates that these modes
 114 are produced by tropospheric baroclinic instability.

115 Although we cannot rule out the possibility of a contribution from synoptic wave-wave
 116 interaction in the control run, the similarity of long-wave characteristics in the control and

117 truncated runs suggests that tropospheric baroclinic instability is the dominant long-wave
118 generation mechanism in both cases.

119 These results reinforce Hartmann's suggestion that traveling planetary waves observed
120 especially in the Southern Hemisphere stratosphere may be the product of tropospheric
121 baroclinic instability rather than of nonlinear interaction between synoptic-scale eddies.

122 **Acknowledgments.** We thank Gang Chen for modeling advice. This work is sup-
123 ported by the National Science Foundation under grant No. 0808831.

References

- 124 Charney, J. and P. Drazin, 1961: Propagation of planetary-scale disturbances from the
125 lower into the upper atmosphere. *J. Geophys. Res.*, **66**.
- 126 Hartmann, D., 1979: Baroclinic instability of realistic zonal-mean states to planetary
127 waves. *J. Atmos. Sci.*, **36**, 2336–2349.
- 128 Held, I. and M. Suarez, 1994: A proposal for the intercomparison of the dynamical cores
129 of atmospheric general circulation models. *BAMS*, **75**, 1825–1830.
- 130 Kushner, P. and L. M. Polvani, 2005: A very large, spontaneous stratospheric sudden
131 warming in a simple AGCM: A prototype for the southern hemisphere warming of
132 2002? *J. Atmos. Sci.*, **62**, 890–897.
- 133 Polvani, L. and P. Kushner, 2002: Tropospheric response to stratospheric perturbations
134 in a relatively simple general circulation model. *Geophys. Res. Lett.*, **29**.
- 135 Scinocca, J. F. and P. Haynes, 1998: Dynamical forcing of stratospheric planetary waves
136 by tropospheric baroclinic eddies. *J. Atmos. Sci.*, **55**, 2361–2392.

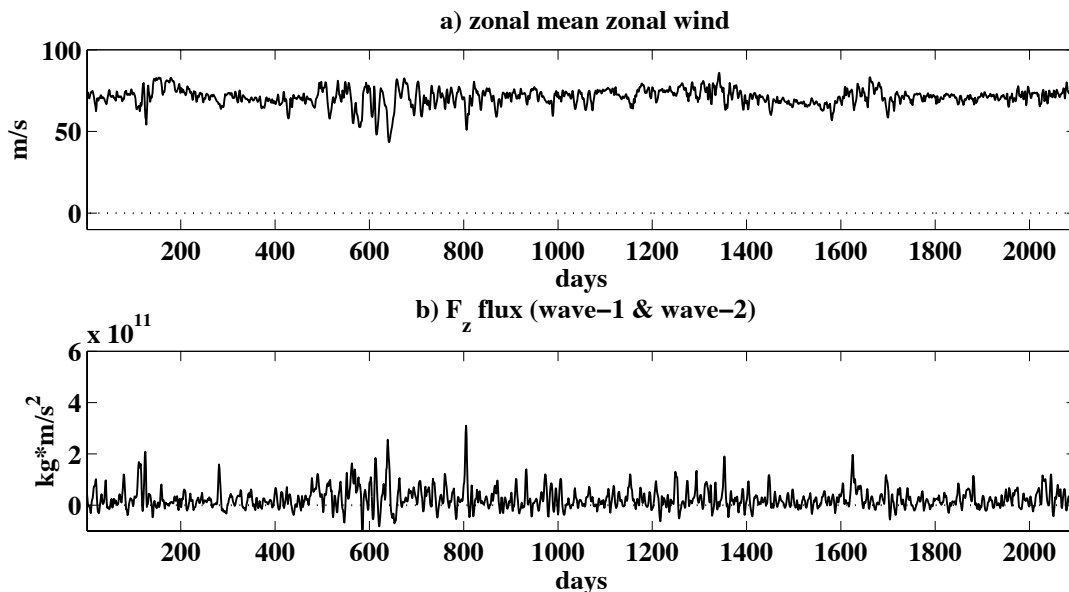


Figure 1. Control run: a) Representative part of the timeseries of zonal mean zonal wind at 60°S and 10hPa in m/s. b) Zonally averaged heat flux for wave-1 and wave-2 at 96hPa for the same time period, integrated between 20° and 70°S according to $\int_{20^{\circ}S}^{70^{\circ}S} F_z \cos(\theta) a d\theta$ where F_z is the vertical component of the Eliassen-Palm flux in spherical coordinates, θ is latitude and a is the Earth’s radius.

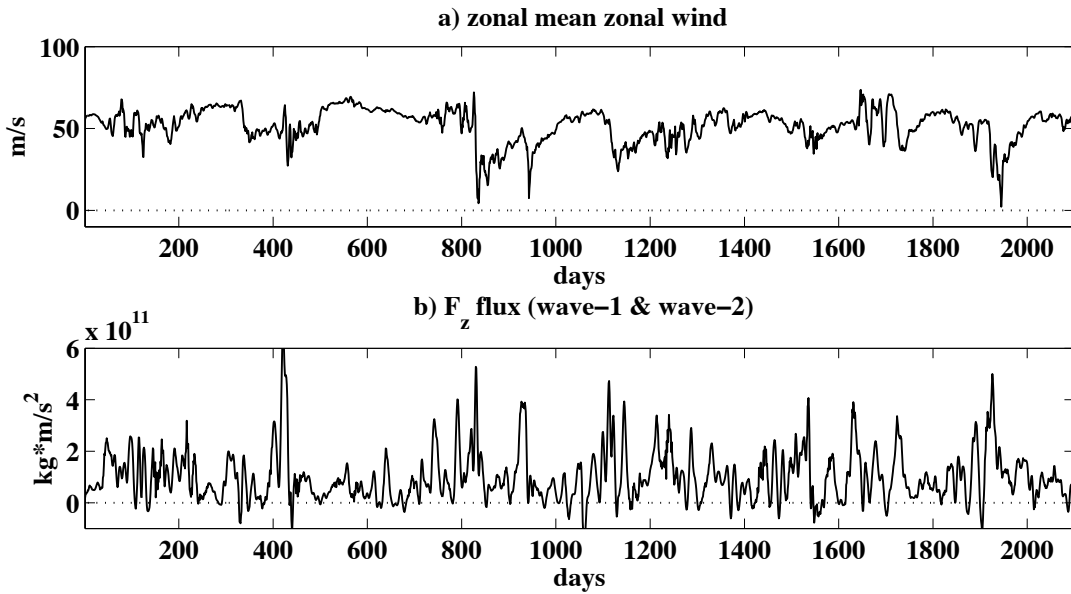


Figure 2. Truncated run: a) Representative part of the timeseries of zonal mean zonal wind at 60°S and 10hPa in m/s . b) Zonally averaged heat flux for wave-1 and wave-2 at 96hPa integrated between 20° and 70°S as for the control run, computed as in Figure 1b.

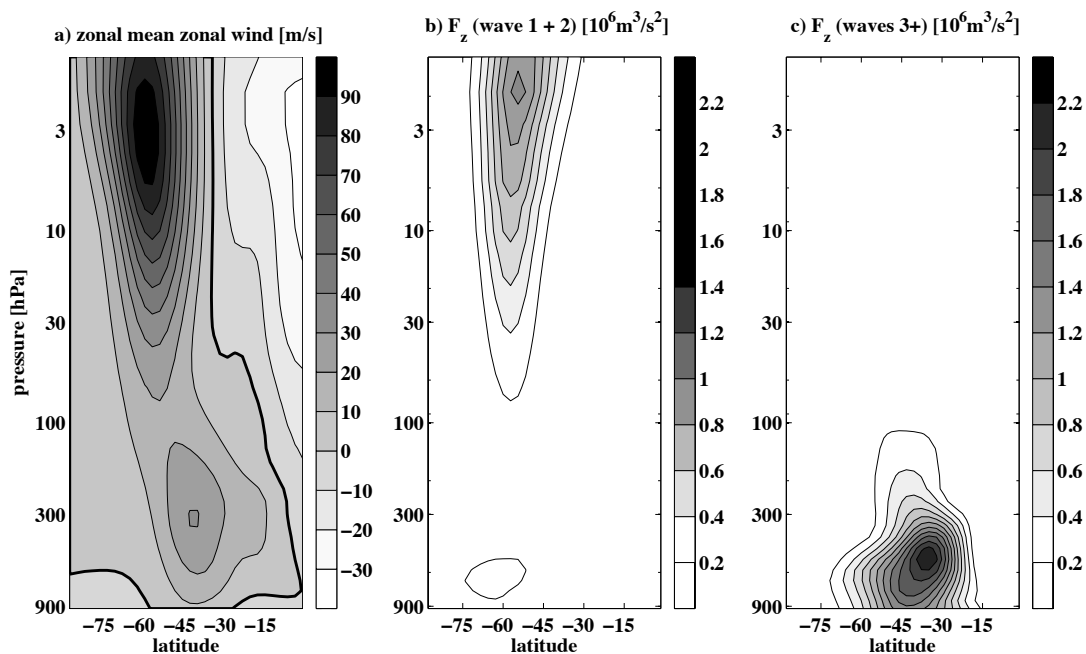


Figure 3. Control run: a) Zonal mean zonal wind averaged over the entire run. Contour interval: 10m/s. Zero wind line printed in bold. b) Vertical component of the Eliassen-Palm Flux (F_z) scaled with density, sum of both propagating waves 1 and 2. Units in $10^6 \text{ m}^3 \text{ s}^{-2}$. Contour interval: $2 \cdot 10^5 \text{ m}^3 \text{ s}^{-2}$ with contours starting at $2 \cdot 10^5 \text{ m}^3 \text{ s}^{-2}$. Zero and negative contours omitted for clarity. c) Same as b) but for wave numbers 3 and higher.

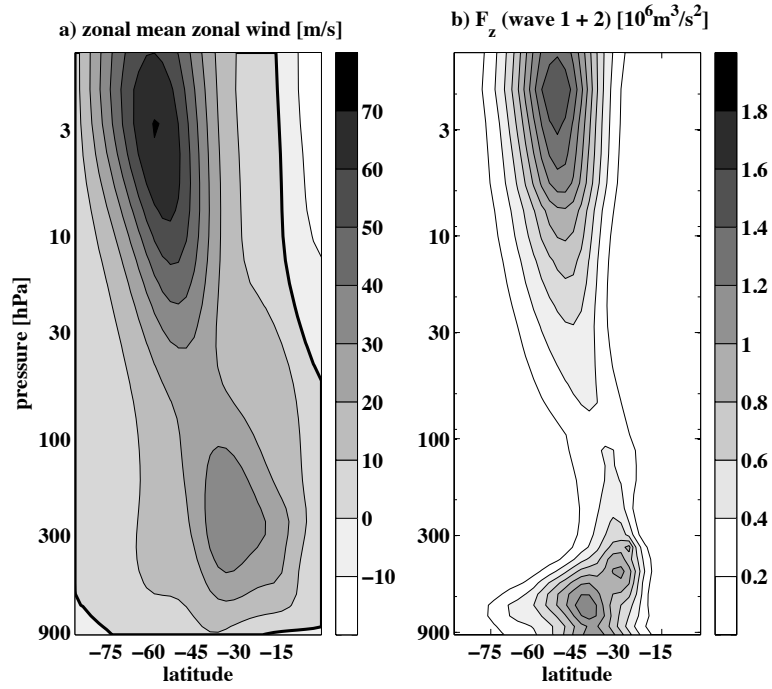


Figure 4. Truncated run (wave-1 and wave-2 only): a) Zonal mean zonal wind averaged over the entire run. Contour interval: 10m/s. Zero wind line printed in bold. b) Vertical component of the Eliassen-Palm Flux (F_z) scaled with density, sum of both propagating waves 1 and 2. Units and contours as in Figure 3.

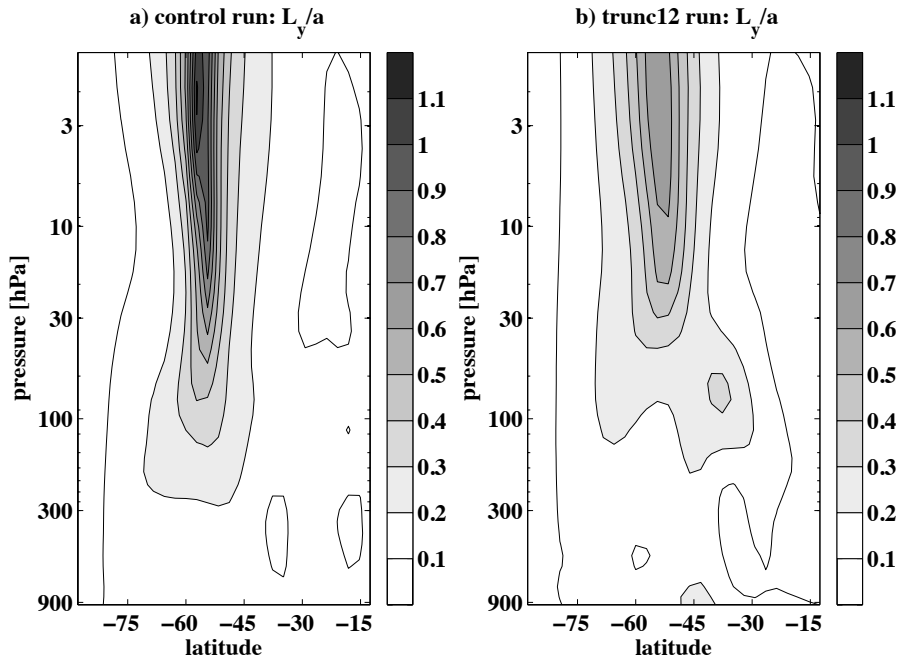


Figure 5. a) L_y/a for zonal wave-2 as a measure of the meridional length scale of the wave in latitude and height as described in equation (1) for the control run. b) Same as figure a) but for the run truncated to wave-1 and wave-2. Contour interval: 0.1 for both figures.

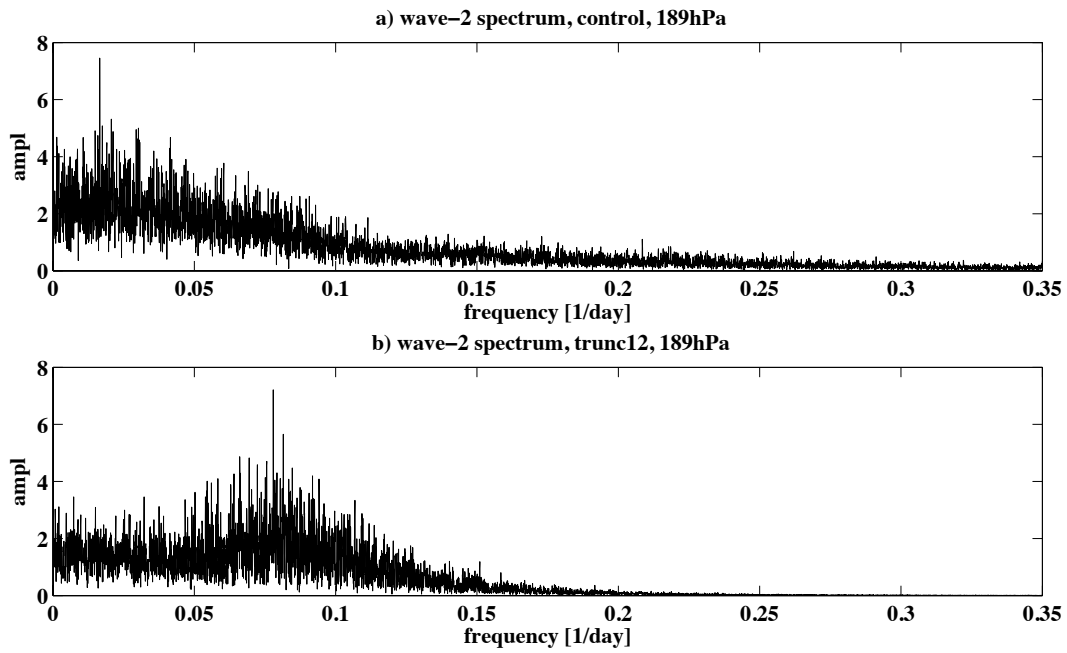


Figure 6. a) Frequency spectrum of geopotential height amplitude for zonal wave-2 at $189hPa$, averaged in longitude, for the control run. b) Same as figure a) but for the run truncated to wave-1 and wave-2.